



## Effect of Calcium Ion Concentration on Small Molecule Desorption from Alginate Beads

Gülşen Akin Evingür, Hakan Kaygusuz, F. Bedia Erim & Önder Pekcan

To cite this article: Gülşen Akin Evingür, Hakan Kaygusuz, F. Bedia Erim & Önder Pekcan (2014) Effect of Calcium Ion Concentration on Small Molecule Desorption from Alginate Beads, Journal of Macromolecular Science, Part B, 53:7, 1157-1167, DOI: [10.1080/00222348.2014.895625](https://doi.org/10.1080/00222348.2014.895625)

To link to this article: <https://doi.org/10.1080/00222348.2014.895625>



Accepted author version posted online: 04 Mar 2014.  
Published online: 17 Jul 2014.



Submit your article to this journal [↗](#)



Article views: 132



View related articles [↗](#)



View Crossmark data [↗](#)



Citing articles: 4 View citing articles [↗](#)

## Effect of Calcium Ion Concentration on Small Molecule Desorption from Alginate Beads

GÜLŞEN AKIN EVINGÜR,<sup>1</sup> HAKAN KAYGUSUZ,<sup>2</sup>  
F. BEDIA ERIM,<sup>2</sup> AND ÖNDER PEKCAN<sup>3</sup>

<sup>1</sup>Faculty of Science and Letters, Piri Reis University, Tuzla- Istanbul, Turkey

<sup>2</sup>Faculty of Science and Letters, Istanbul Technical University, Maslak- Istanbul, Turkey

<sup>3</sup>Faculty of Engineering and Natural Sciences, Kadir Has University, Cibali- Istanbul, Turkey

*Spherical alginate beads were prepared by ionotropic gelation of sodium alginate through the use of calcium ions. Pyranine (Py) was added to the alginate solution as a small molecule probe for fluorescence studies. Desorption of Py in water from the alginate beads cross-linked with calcium ions was studied by using the steady state fluorescence technique. The fluorescence emission intensity ( $I$ ) from Py was monitored during the desorption process at 512 nm using the time drive mode of the spectrofluorometer. The increase in  $I$  was attributed to Py release from the beads. The Fickian diffusion model was used to calculate the desorption coefficients,  $D$ , which were found to be increased up to 3% (w/v)  $\text{CaCl}_2$  concentration in the beads, and then decreased with a further increase of  $\text{CaCl}_2$  content. On the other hand, the encapsulation efficiency of Py in the calcium alginate beads presented the reverse behavior compared to  $D$ . It was observed that, when the content of  $\text{CaCl}_2$  was increased, the incubation time,  $t_0$ , for the start of desorption increased.*

**Keywords** alginate, desorption,  $\text{CaCl}_2$ , fluorescence, encapsulation efficiency, pyranine

### Introduction

Alginate acid is a biopolymer consisting of homopolymeric blocks of (1–4)-linked  $\beta$ -D-mannuronate and  $\alpha$ -L-guluronate. The anionic form of alginate acid, alginate, is widely used in various areas, including controlled release systems,<sup>[1,2]</sup> food applications,<sup>[3]</sup> water purification agents,<sup>[4]</sup> and many other industrial applications. Alginate acid forms stable gels as metals interact ionically with blocks of uronic acid residues, resulting in the formation of a three-dimensional network that is usually described as an “egg-box” structure.<sup>[5,6]</sup> In the case of beads prepared from pure sodium alginate, the formation of beads takes place due to ionotropic gelation of spherical drops. The polyguluronate units in the alginate molecules form a chelated structure with metal ions, called an “egg-box” junction with interstices in

Received 26 July 2013; accepted 7 January 2014.

Address correspondence to Gülşen Akin Evingür, Piri Reis University, Faculty of Science and Letters, 34940, Tuzla- Istanbul, Turkey. E-mail: gulsen.evingur@pirireis.edu.tr

Color versions of one or more of the figures in the article can be found online at [www.tandfonline.com/lmsb](http://www.tandfonline.com/lmsb).

which the cations may pack and be coordinated. The junction between the chains formed in this way is kinetically stable toward dissociation while the polymannuronate units show the normal polyelectrolyte characteristics of cation binding.

Calcium ion release from alginate gels is known and has been reported in the literature as it pertains to antibiotics,<sup>[7]</sup> bacteria,<sup>[8]</sup> macromolecular drugs,<sup>[9]</sup> proteins,<sup>[10]</sup> spermatozoa,<sup>[11]</sup> and vitamins.<sup>[12]</sup> The mechanical and functional properties of metal-alginate gels can be modified by adding organic and inorganic compounds to the gel.<sup>[13–15]</sup> In addition, it has been reported that the amount of calcium ions affects the surface morphology, porosity, and drug release behavior.<sup>[16,17]</sup> Fluorescence probes can be used for the testing of these applications. Py is a water-soluble, pH-sensitive, and intrinsic fluorophore. Adding a luminescent dye as a probe makes it possible to measure intracellular pH values<sup>[18]</sup> and proton transfer.<sup>[19]</sup> Py has been used as a fluorescent probe for monitoring the gelation of polyacrylamide-sodium alginate composites and sol-gel transition properties of  $\kappa$ -carrageenan.<sup>[20,21]</sup> The cation effect on the thermal transition of iota carrageenan has been performed by a photon transmission technique,<sup>[22]</sup> and activation energies were found to be strongly correlated to the  $\text{CaCl}_2$  content in the system. The monovalent and divalent cation effects have also been studied as regards the phase transitions of iota carrageenan.<sup>[23]</sup> The steady state fluorescence technique has been used previously to study small molecule diffusion into polyacrylamide at different temperatures,<sup>[24]</sup> iota carrageenan gels,<sup>[25]</sup> sorption and slow release of polyacrylamide,<sup>[26]</sup> and PVA-pyrene chains in and out of agarose gel.<sup>[27]</sup> The Fickian diffusion model was used to quantify the experimental results for each of these materials and it was found that agarose gel possesses two distinct diffusion regions.

In this study, we sought to examine the desorption of Py in water from alginate beads cross-linked with calcium ( $\text{Ca}^{2+}$ ) ions by using the steady state fluorescence technique. Py was added to an alginate solution as a fluorescence probe. The influence of  $\text{CaCl}_2$  concentration on desorption was observed, and Py release kinetics from the alginate beads was investigated by using the Fickian diffusion model. The desorption coefficients,  $D$ , and encapsulation efficiency (EE) were calculated. Additionally, the incubation time,  $t_o$ , for desorption was defined for different  $\text{CaCl}_2$  concentrations and it was observed that as the content of  $\text{CaCl}_2$  was increased,  $t_o$  increased as well, and  $D$  was found to decrease linearly when the EE was increased.

## Materials and Methods

### Materials

Alginic acid sodium salt (Viscosity of  $\sim 250$  cps) was purchased from Sigma-Aldrich Co. (USA), and calcium chloride dehydrate (analytical grade) was obtained from J.T. Baker Co. (Holland). Fluorescence measurements were performed with the use of a Shimadzu RF-5301PC spectrofluorometer (Japan) at room temperature.

### Preparation of Beads

Sodium alginate was dissolved in 5 mL deionized water at a concentration of 2% (w/v), and the Py content was kept constant at  $10^{-4}$  M in the solution. The solution was mixed and left for several hours to eliminate air bubbles. It was then added dropwise through a 0.8 cm inner diameter syringe to a calcium chloride solution of various concentrations (0.5–20% (w/v)). The addition of the alginate/pyranine solution was conducted 20 cm over

the calcium chloride solution vessel in order to produce perfect spherical beads. The formed beads were filtered, washed three times with deionized water to make sure that the Py was completely removed from the surface of the beads and then placed on a Petri dish. The beads had an average diameter of  $2.0 \pm 0.1$  mm.

### Encapsulation

The amount of Py that escaped into the calcium chloride solution and washing water during preparation was determined using the absorption at 290 nm via UV-VIS spectroscopy.<sup>[28]</sup> Py calibration plot procedures were conducted as follows: Various amounts of standard Py calibration solutions were prepared and their absorbances at 445 nm were measured using the Shimadzu UV-1800 spectrometer. After that, the absorbance values of the samples were also measured. EE of Py in the alginate beads was calculated by using Eq. (1)

$$EE (\%) = \frac{n_0 - (n_m + n_w)}{n_0} \times 100, \quad (1)$$

where  $n_o$  is the initial amount of Py, and  $n_m$  and  $n_w$  are the amount of Py in the calcium chloride solution and washing water, following preparation of the beads, respectively. The units are in moles.

### Desorption

Suitable amounts of wet beads were placed at the bottom of a quartz cuvette in order to create a single layer structure. After 1 mL of deionized water was added without disturbing this single layer, the cuvette was immediately placed into the spectrofluorometer. The position of the single layer alginate beads in the cuvette with and without  $10^{-4}$  M Py before and after desorption are given in Figs. 1(a) and 1(b), respectively. Excitation wavelength

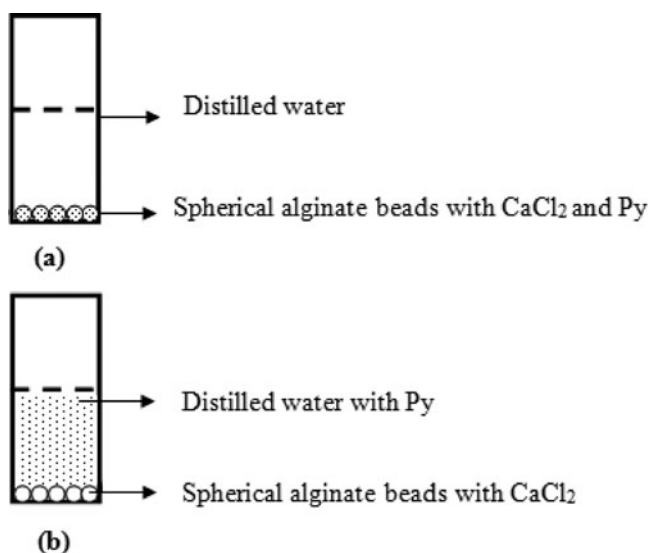


**Figure 1.** Position of alginate beads with Py on the bottom of the fluorescence cuvette (a) before and (b) after desorption process.

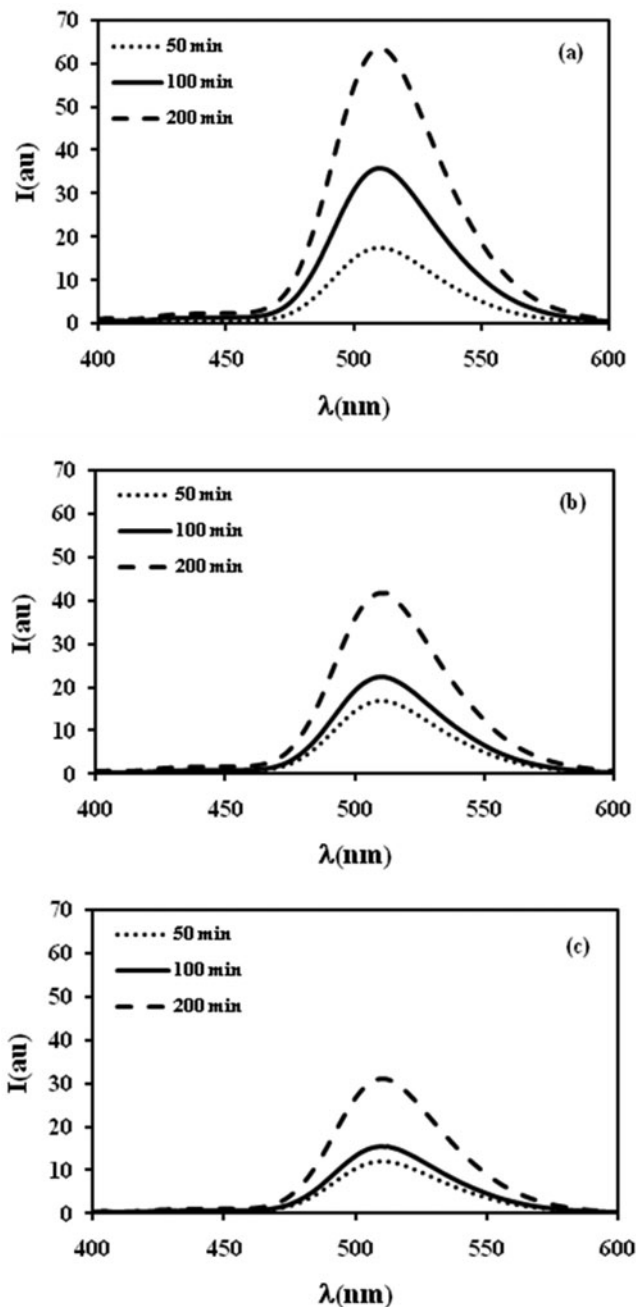


**Figure 2.** Fluorescence spectra of Py desorbed into water from the beads cross-linked with (a) 1, (b) 5, and (c) 20% (w/v)  $\text{CaCl}_2$  solution, respectively, at 50, 100, and 200 min.

and fluorescence emission wavelength were set to 340 and 512 nm, which were used to monitor the Py desorption into the desorption media (water) using the time-drive mode of the spectrofluorometer. At the end of the measurement, the cuvette was taken out and shaken well in order to let the Py diffuse completely into the water. At this point, the

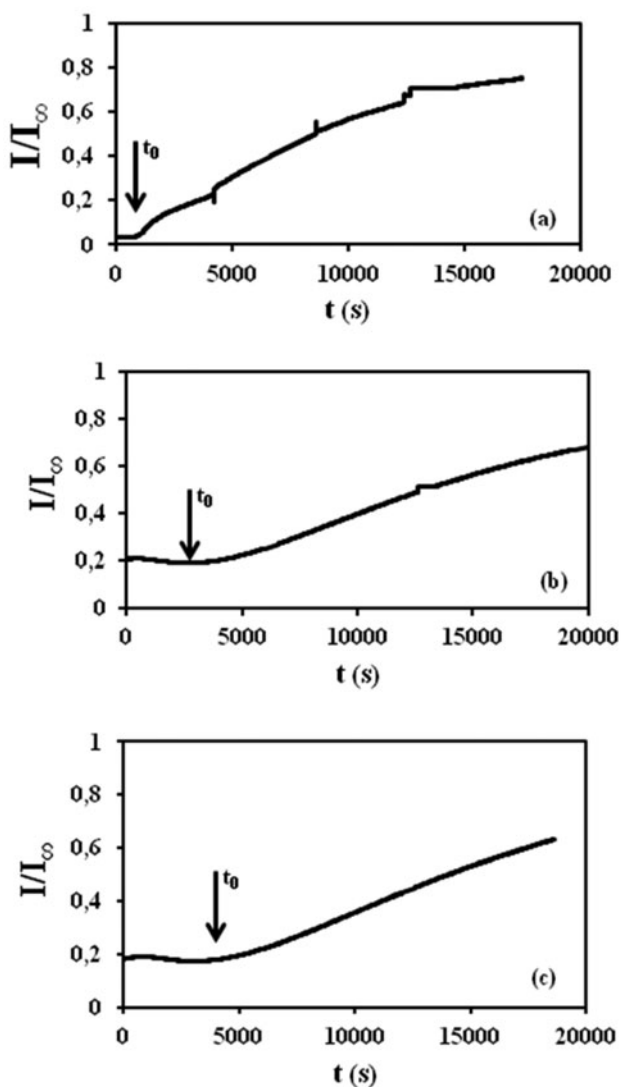


**Figure 3.** Normalized fluorescence intensity at 512 nm,  $I/I_{\infty}$ , versus time for the beads cross-linked with (a) 1, (b) 5, and (c) 20% (w/v)  $\text{CaCl}_2$  solution, respectively.

final fluorescence intensity ( $I_{\infty}$ ) of the solution was measured to normalize the emission intensities,  $I$ . The Py increased into the water linearly and nearly saturated as the Py was released from the beads.

### *Fickian Model*

The mathematical theory of diffusion in isotropic substances is based on the hypothesis that the rate of transfer of diffusing substances through the unit area of a section is proportional to the concentration gradient measured normal to the section, i.e.,

$$F = -D \frac{\partial C}{\partial z}, \quad (2)$$

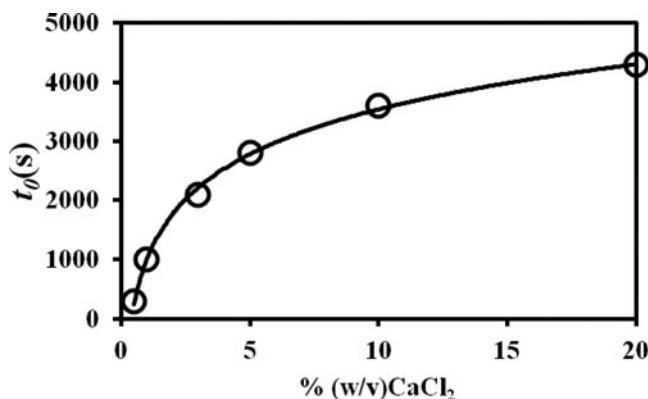


**Figure 4.** Incubation time  $t_0$ (s) versus % (w/v) CaCl<sub>2</sub> solution content.

where  $F$  is the rate of transfer per unit area of the section,  $C$  is the concentration of diffusing substance,  $z$  is the space coordinate measured normal to the section, and  $D$  is called the diffusion coefficient. In the case of diffusion in dilute solutions,  $D$  can reasonably be taken as constant. The negative sign in Eq. (2) arises because diffusion occurs in the direction opposite to that of increasing concentration. From Eq. (2), by using simple geometric considerations, the differential equation of diffusion in one dimension can be derived as:

$$\frac{\partial C}{\partial t} = D \frac{\partial^2 C}{\partial z^2}. \quad (3)$$

Eqs. (2) and (3) are usually referred to as Fick's first and second laws. Diffusion occurs just in the  $z$  direction. When the boundary is kept at a constant concentration,  $C_0$ , the initial concentration being zero throughout the medium. Eq. (3) satisfies the boundary conditions which for  $t = 0$  at  $z = 0$ ,  $C = 0$  and for  $t \geq 0$ , at  $z = a$ ,  $C = C_0$ .

**Table 1**

Experimentally measured parameters for the beads cross-linked with various % (w/v) CaCl<sub>2</sub> solution

% (w/v) CaCl <sub>2</sub> solution	Initial height* (mm)	Incubation time, $t_0$ (s)	Encapsulation efficiency of pyranine (%)	Desorption coefficient, $D^*10^{-12}$ (m <sup>2</sup> /s)
0.5	2.0	300	16.92	62.17
1	2.0	1000	25.15	59.41
3	2.0	2100	42.48	52.78
5	2.0	2800	52.18	47.75
10	2.0	3600	59.84	42.98
20	2.0	4300	63.52	41.83

\*Equals bead's diameter.

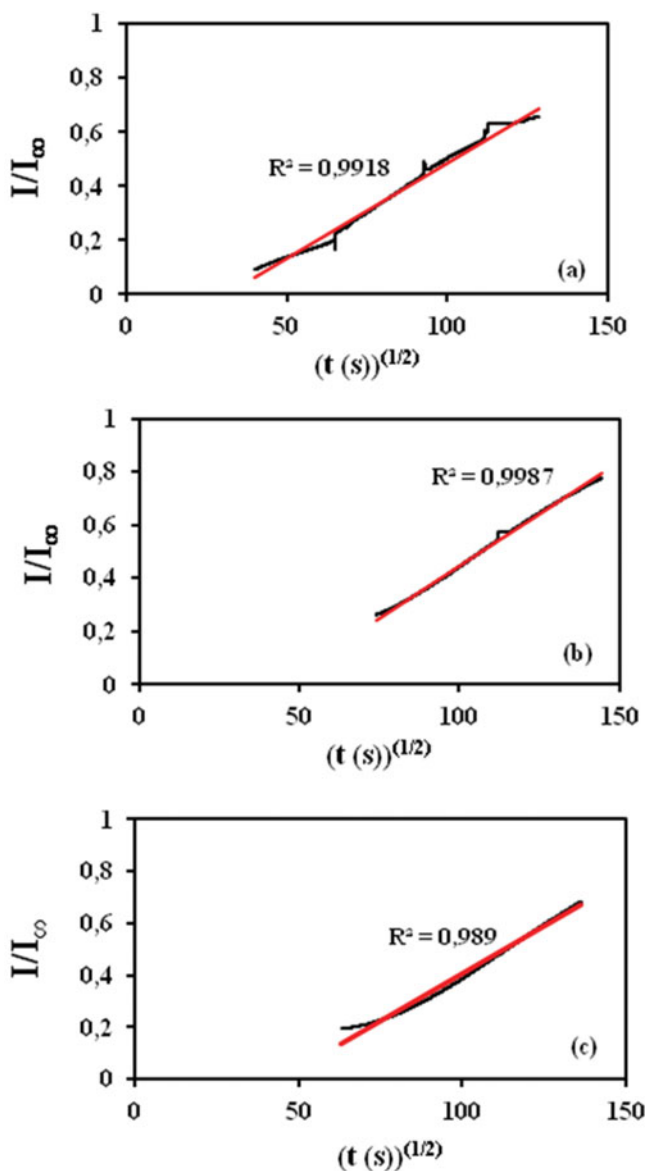


**Figure 5.** Fit of the desorption data in Fig. 3 according to Eq. (5) for the beads cross-linked with (a) 1, (b) 5, and (c) 20% (w/v) CaCl<sub>2</sub> solution, respectively.

Eq. (3) can be solved as:

$$\frac{M_t}{M_\infty} = \frac{4}{\pi^{1/2}} \left(\frac{Dt}{a^2}\right)^{1/2} - \frac{Dt}{a^2} - \frac{1}{3\pi^{1/2}} \left(\frac{Dt}{a^2}\right)^{3/2} + \dots \quad (4)$$

where  $M_t$  and  $M_\infty$  are the amount of material diffused in time  $t$  and at equilibrium, respectively, and  $a$  represents the thickness of the disc shape structure.<sup>[29]</sup>



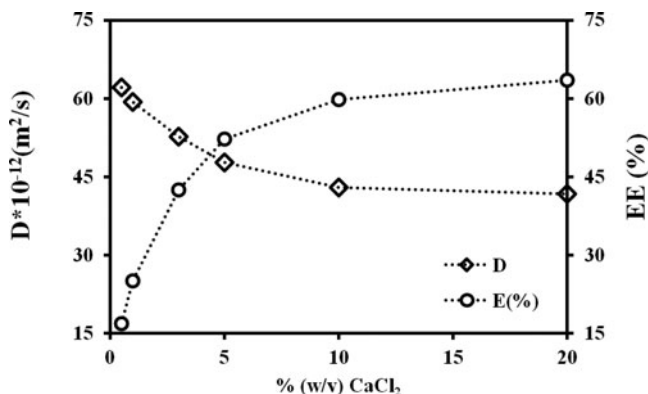


**Figure 6.** Desorption coefficients  $D$  and encapsulation efficiency (EE) versus various % (w/v)  $\text{CaCl}_2$  solution, respectively.

## Results and Discussion

The typical fluorescence spectra of Py desorbed into water from the alginate beads cross-linked with 1%, 5%, and 20% (w/v)  $\text{CaCl}_2$  solutions at various times are presented in Fig. 2(a)–(c), respectively.

During desorption experiments, one should expect an increase in fluorescence intensity at 512 nm due to the increasing amount of free Py molecules in the water, as presented in Fig. 2. In order to quantify the behavior of  $I$  at early times, Eq. (4) can be written in the following way:

$$\frac{I}{I_\infty} = \frac{4}{\pi^{1/2}} \left( \frac{Dt}{a^2} \right)^{1/2}. \quad (5)$$

Here, it is assumed that the amount of desorbed pyranine molecules,  $M_t$  and  $M_\infty$ , are proportional to  $I$  and  $I_\infty$ . The fluorescence intensities at 512 nm which were measured versus time are shown in Fig. 3(a)–(c) for the alginate beads cross-linked with 1%, 5%, and 20% (w/v)  $\text{CaCl}_2$  solutions, respectively.

The Py intensity,  $I$ , during desorption, were normalized according to the highest intensity,  $I_\infty$ , at the longest time. It was seen that the fluorescence intensity increased, indicating that Py molecules were released gradually from the beads cross-linked with various calcium ion contents as the desorption time was increased. The curves in Fig. 3 show typical desorption behavior, and the desorption process can be treated using the Fickian diffusion model. It is interesting to note that the desorption process starts after a certain time, called the incubation time,  $t_0$ , at which desorption just starts to increase. It is the time required for the beads to absorb enough water and mobilize Py in the bead before Py desorption starts. Figure 4 shows the variation of  $t_0$  versus calcium ion content in the solutions; they are also listed in Table 1. As can be seen in Fig. 4, when the calcium ion content was increased,  $t_0$  increased as expected, due to the degree of cross-linking in the alginate beads, i.e., more ions create stronger gels which kept the Py molecules in the alginate beads, resulting in a delay in the desorption process because of the egg-box junction of  $\text{Ca}^{2+}$  ions.<sup>[5–6]</sup> That indicates a higher amount of cross-linking is related to amount of  $\text{Ca}^{2+}$  ions.

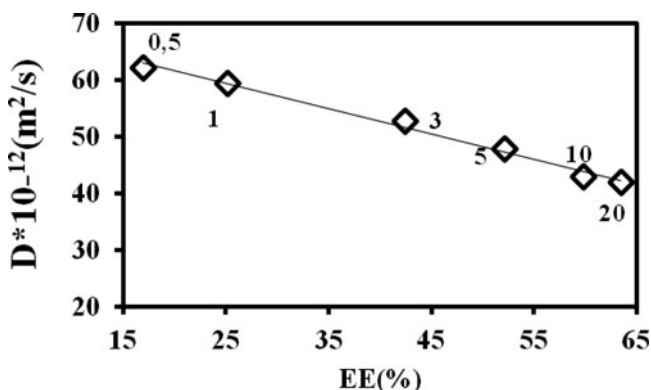


**Figure 7.** Desorption coefficients  $D$  versus EE for various% (w/v)  $\text{CaCl}_2$  solution.

The fits of normalized fluorescence intensities by using Eq. (5) are shown as a function of time in Fig. 5(a)–(c) for the beads cross-linked with 1%, 5%, and 20% (w/v)  $\text{CaCl}_2$  solutions, respectively; they produced the desorption coefficients,  $D$ , which are listed in Table 1.

The  $D$  values decreased and the EE of Py in the calcium alginate beads showed the reverse behavior with increasing  $\text{CaCl}_2$ , presented in Fig. 6 and given in Table 1. The EEs were obtained in the range of 16.92–63.52%; the beads cross-linked with 0.5% (w/v)  $\text{CaCl}_2$  solution gave the lowest EE% of 16.92% and the beads cross-linked with 20% (w/v)  $\text{CaCl}_2$  solution resulted in the highest EE% of 63.52%.

To interpret the above results, the desorption coefficients and EE versus (w/v)  $\text{CaCl}_2$  solution content are plotted in Fig. 7, where it is seen that the desorption coefficients decreased<sup>[30]</sup> as EE increased, indicating that the total Py released from the beads decreased as the EE of the beads increased. The removal of the Py molecules in the beads cross-linked with 0.5% (w/v)  $\text{CaCl}_2$  solution showed the lowest EE and the highest desorption coefficient. On the other hand, the Py release from beads cross-linked with a 20% (w/v)  $\text{CaCl}_2$  solution was the lowest, leading to the greatest EE and the smallest desorption coefficient. In other words, the highest EE produced the lowest  $D$ . It could be explained by the fact as expected, that the use of higher  $\text{CaCl}_2$  solution would increase the cross-linking of the beads, increasing the EE, and delaying the release.

## Conclusions

In this study, we calculated and compared the desorption coefficients with the encapsulation efficiencies in alginate beads cross-linked with various% (w/v)  $\text{CaCl}_2$  solutions. The steady state fluorescence method combined with the Fickian diffusion model was employed to produce desorption coefficients. It was seen that increasing the calcium ion concentration in the beads led to a decrease in the desorption coefficient and an increase in the EE of the calcium alginate beads. The results showed that the highest% (w/v)  $\text{CaCl}_2$  concentration produced the lowest desorption coefficient for the beads, which can be explained in terms of the increasing of cross-linking in the beads and the egg-box junction structure of  $\text{Ca}^{2+}$  ions.

## Acknowledgment

Experiments were carried out in the Spectroscopy Laboratory of the Department of Molecular Biology and in the Capillary Electrophoresis Laboratory of the Department of Chemistry at Istanbul Technical University.

## References

1. Kikuchi, A.; Kawabuchi, M.; Sugihara, M.; Sakurai, Y.; Okano, T. Pulsed dextran release from calcium-alginate gel beads. *J. Control. Rel.* **1997**, *47*, 21.
2. Işıklan, N.; İnal, M.; Kurşun, F.; Ercan, G. pH responsive itaconic acid grafted alginate microspheres for the controlled release of nifedipine. *Carbohydr. Polym.* **2011**, *84*, 933.
3. Bierhalz, A.C.K.; Silva, M.A.; Kieckbusch, T.G. Natamycin release from alginate/pectin films for food packaging applications. *J. Food Eng.* **2012**, *110*, 18.
4. Banerjee, A.; Nayak, D.; Lahiri, S. Speciation-dependent studies on removal of arsenic by iron-doped calcium alginate beads. *Appl. Radiat. Isot.* **2007**, *65*, 769.
5. Papageorgiou, S.K.; Kouvelos, E.P.; Favvas, E.P.; Sapalidis, A.A.; Romanos, G.E.; Katsaros, F.K. Metal-carboxylate interactions in metal-alginate complexes studied with FTIR spectroscopy. *Carbohydr. Res.* **2010**, *345*, 469.
6. Grant, G.T.; Morris, E.R.; Rees, D.A.; Smith, P.J.C.; Thom, D. Biological interactions between polysaccharides and divalent cations: The egg-box model. *FEBS Lett.* **1973**, *32*, 195.
7. Anal, A.K.; Stevens, W.F. Chitosan-alginate multilayer beads for controlled release of ampicillin. *Int. J. Pharm.* **2005**, *290*, 45.
8. Cook, M.T.; Tzortzis, G.; Charalampopoulos, D.; Khutoryanskiy, V.V. Microencapsulation of probiotics for gastrointestinal delivery. *J. Control. Rel.* **2012**, *162*, 56.
9. Chretien, C.; Chaumei, J.C. Release of a macromolecular drug from alginate-impregnated microspheres. *Int. J. Pharm.* **2005**, *304*, 18.
10. Nochos, A.; Douroumis, D.; Bouropoulos, N. In vitro release of bovine serum albumin from alginate/HPMC hydrogel beads. *Carbohydr. Polym.* **2008**, *74*, 451.
11. Torre, M.L.; Maggi, L.; Vigo, D.; Galli, A.; Bornaghi, V.; Maffeo, G.; Conte, U. Controlled release of swine semen encapsulated in calcium alginate beads. *Biomater.* **2000**, *21*, 1493.
12. Abd El-Ghaffar, M.A.; Hashem, M.S.; El-Awady, M.K.; Rabie, A.M. pH-sensitive sodium alginate hydrogels for riboflavin controlled release. *Carbohydr. Polym.* **2012**, *89*, 667.
13. Pasparakis, G.; Bouropoulos, N. Swelling studies and in vitro release of verapamil from calcium alginate and calcium alginate-chitosan beads. *Int. J. Pharm.* **2006**, *323*, 34.
14. Zhang, H.; Gao, X.; Guo, T.; Li, Q.; Liu, H.; Ye, X.; Guo, M.; Wu, Z. Adsorption of iodide ions on a calcium alginate-silver chloride composite adsorbent. *Colloids Surf. A* **2011**, *386*, 166.
15. Tezcan, F.; Günster, E.; Özen, G.; Erim, F.B. Biocomposite films based on alginate and organically modified clay. *Int. J. Biol. Macromol.* **2012**, *50*, 1165.
16. Pathak, T.S.; Yun, J-H.; Lee, J.; Paeng, K-J. Effect of calcium ion (cross-linker) concentration on porosity, surface morphology and thermal behavior of calcium alginates prepared from algae (*Undaria pinnatifida*). *Carbohydr. Polym.* **2010**, *81*, 633.
17. Pongjanyakul, T.; Puttipatkhachorn, S. Modulating drug release and matrix erosion of alginate matrix capsules by microenvironmental interaction with calcium ion. *Eur. J. Pharm. Biopharm.* **2007**, *67*, 187.
18. Gan, B.S.; Krump, E.; Shrode, L.D.; Grinstein, S. Loading pyranine via purinergic receptors or hypotonic stress for measurement of cytosolic pH by imaging. *Am. J. Physiol. Cell. Physiol.* **1998**, *275*, C1158-C1166.
19. Mondal, S.K.; Sahu, K.; Sen, P.; Roy, D.; Ghosh, S.; Bhattacharyya, K. Excited state proton transfer of pyranine in a  $\gamma$ -cyclodextrin cavity. *Chem. Phys. Lett.* **2005**, *412*, 228.
20. Evingür, G.A.; Tezcan, F.; Erim, F.B.; Pekcan, Ö. Monitoring the gelation of polyacrylamide-sodium alginate composite by fluorescence technique. *Phase Transit.* **2012**, *85*, 530.

21. Pekcan, Ö.; Tari, Ö. A fluorescence study on the gel-to-sol transition of  $\kappa$ -carrageenan. *Int. J. Bio. Macromol.* **2004**, *34*, 223.
22. Pekcan, Ö.; Kara, S. Cation effect on thermal transition of iota-carrageenan: A photon transmission study. *J. Biomater. Sci. Polym. Ed.* **2005**, *16*, 317.
23. Kara, S.; Arda, E.; Pekcan, Ö. Monovalent and Divalent Cation Effects on Phase Transitions of  $\iota$ -carrageenan. *J. Bioact. Compat. Polym.* **2007**, *22*, 42.
24. Evingür, G.A.; Karlı, K.; Pekcan, Ö. Monitoring small molecule diffusion into hydrogels at various temperatures by fluorescence technique. *Int. J. Pharm.* **2006**, *326*, 7.
25. Ataman, E.; Pekcan, Ö. Small molecule diffusion into swelling Iota-Carrageenan gels: A fluorescence study. *J. Biomol. Struct. Dyn.* **2007**, *24*, 505.
26. Evingür, G.A.; Pekcan, Ö. Sorption and slow release kinetics of PAAm gels at various temperatures. *J. Polym. Eng.* **2007**, *27*, 583.
27. Kara, S.; Gacal, B.; Tunç, D.; Yağcı, Y.; Pekcan, Ö. Sorption and desorption of PVA-Pyrene Chains in and out of Agarose gel. *J. Fluoresc.* **2012**, *22*, 1073.
28. Ashokkumar, M.; Grieser, F. Sono Photoluminescans: Pyranine emission induced by ultrasound. *J. Chem. Soc. Chem. Commun.* **1998**, 561–562.
29. Crank, J, *The Mathematics of Diffusion*. Clarendon Press: Oxford, **1975**.
30. Akihiko, K.; Minako, K.; Atsushi, W.; Masayasu, S.; Yasuhisa, S.; Teruo, O. Effect of  $\text{Ca}^{2+}$ -alginate gel dissolution on release of dextran with different molecular weights. *J. Control. Rel.* **1999**, *58*, 21.